ASEAN Engineering Journal

Full Paper

OPTIMIZATION OF MATHEMATICAL MODELING OF MICROBIAL ELECTROLYSIS CELL FOR THE PRODUCTION OF HYDROGEN FROM SAGO WASTEWATER SUBSTRATE

Mohamad Afiq Mohd Asrul[a], Mohd Farid Atan[a,b,c,d], Hafizah Abdul Halim Yun[a,e*], Noraziah Abdul Wahab[a,b,c,d], Hu Hin Hung[a], Josephine Chang Hui Lai [a,b], Ivy Ai Wei Tan[a]

[a]Department of Chemical Engineering and Energy Sustainability, Faculty of Engineering, Universiti Malaysia Sarawak, 94300, Kota Samarahan, Sarawak, Malaysia.
[b]Institute of Sustainable and Renewable Energy (ISuRE), Universiti Malaysia Sarawak, 94300, Kota Samarahan, Sarawak, Malaysia.
[c]Institute of Social Informatics and Technological Innovations (ISITI), Universiti Malaysia Sarawak, 94300, Kota Samarahan, Sarawak, Malaysia.
[d]University Sustainability Centre, Universiti Malaysia Sarawak, 94300, Kota Samarahan, Sarawak, Malaysia.
[e]Centre for Applied Learning and Multimedia, Universiti Malaysia Sarawak, 94300, Kota Samarahan, Sarawak, Malaysia.

Article history
Received
18 May 2023
Received in revised form
30 October 2023
Accepted
07 November 2023
Published online
31 May 2024

*Corresponding author
ahyhafizah@unimas.my

Graphical abstract

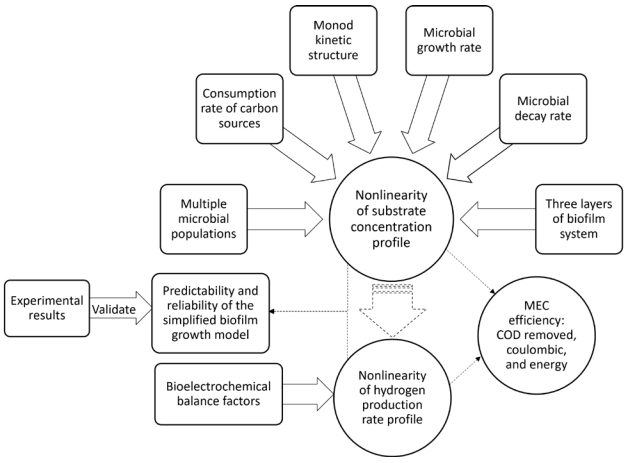

Abstract

The experimental runs of a 4-L double-chamber microbial electrolysis cell (MEC) produce hydrogen from sago wastewater within the retention time of 16 days. The simulation of the simplified microbial biofilm growth model provides the results to validate the experimental data. However, the comparable profiles have a nonlinear phenomenon, such as the data deviation in substrate concentration and hydrogen production rate. The stoichiometric reaction and kinetics affect the behavior of the substrate concentration profile. In addition, the bioelectrochemical factors also affect the hydrogen production rate profile. The artificial neural network (ANN) predicts the experimental hydrogen production rate according to the input of pH of the catholyte at controlled applied potential of 0.8 V and current density of 0.632 $A \cdot m^{-2}$. The convex method assists the model in finding the optimal input values that lead to the minimum mean square error (MSE) between modelling and experimental data. Evaluation of the COD removal efficiency, coulombic efficiency, and energy efficiency determines the process limit of the model MEC. At an optimum applied potential of 0.45 V, anode surface area of 0.06 m^2, anodic chamber volume of 5.2 L, and initial substrate concentration of 2,476.14 $mg \cdot L^{-1}$, the MEC model reached maximum steady-state percentage at 100.0% of COD removal efficiency, 50.0% of Coulombic efficiency, and 7.8% of energy efficiency.

Keywords: Biohydrogen, microbial electrolysis cell, biofilm growth, artificial neural network, mathematical model, optimization

1.0 INTRODUCTION

A microbial electrolysis cell (MEC) is an integrated fermentation redox reactor for the production of hydrogen from a variety of organic wastewaters with very low energy input [1–6]. However, current performance has not yet reached the point where it can be realized on a large scale [7]. The anaerobic environment of the anodic chamber could prevent the MEC from producing oxygen gas and electricity to ensure that hydrogen gas is the final product in the cathodic chamber [1, 2, 6]. Adopting a dual-chamber configuration could effectively minimize the tendency for methane emissions during the microbial reaction [8]. The excellent energy efficiency of sago wastewater as a substrate in MEC processes has been scientifically demonstrated [9], which is due to its typical composition with high sugar content. Otherwise, direct discharge without proper treatment may negatively affect the aquatic ecosystem of the river, especially by changing the pH of the water and groundwater quality [10–13].

The bioelectrochemical reaction of hydrogen from fermentation of wastewater, also known as substrate in MEC [2], is subject to nonlinearity, and the interactions for several variables are complex [14]. All these complexities could be related to the fact that the variation of dynamic bacterial activity causes the nonlinear effect of biohydrogen production [3]. The modeling technique seems promising to overcome the existing limitations of experimental analysis [3, 4, 15].

The dynamic phenomena of the bioelectrochemical process in the MEC have been critically analyzed in many studies using a simplified model of microbial biofilm growth based on the assumptions of Pinto et al. [16]. Statistical analysis of MEC processing of sago mill wastewater substrate to hydrogen gas using response surface methodology (RSM) has been reported previously [17]. However, nonlinearity occurred in laboratory runs of batch MEC fed sago wastewater in 16 retention days. This was related to the significant deviation between the experimental data and the comparable results from the simulated mathematical model. Substrate concentration was measured by the COD of the anolyte. The hydrogen production rate was indicated by the pH drop of the catholyte.

The variation of the input values of the stochiometric reaction and kinetics parameters and the changes in the initial values of the state variables had a significant effect on the substrate concentration profile [6, 18], and these uncertainty parameters could not be adjusted or controlled in the experiment. On the other hand, the perturbation value of the applied potential has a direct effects on the hydrogen production rate [14]. The underestimation of the hydrogen production profile in certain process time intervals is indirectly influenced by the stochiometric reaction and kinetic factors that affect the MEC current with respect to the microbial equilibrium concentrations [19]. As far as the authors are aware, no optimization of the model has been performed in the literature to minimize the data variance of substrate concentration and hydrogen production rate due to the aforementioned nonlinear interactions of the various input factors.

Unlike the substrate concentration data, the hydrogen production rate data were measured in pH values that require unit conversion. The relationship between catholyte pH and hydrogen production rate with multivariate effects of current density and applied potential [20] was complex to correlate, but it is possible to do so with the application of artificial intelligence algorithms capable of deriving a mathematical equation from artificial neural networks (ANN) data learning.

The main objective of the research is to improve the validity and reliability of the simplified biofilm growth model for the purpose of optimizing the laboratory MEC process for biohydrogen production from sago wastewater. MATLAB (R2022a software license number: 40774331) was accessed to achieve the following sub-objectives: (i) to validate the mathematical modeling results of the substrate concentration profile and hydrogen production rate profile using the data from the MEC experiment on biohydrogen production from sago wastewater substrate, and (ii) to determine the process limit of MEC by maximizing the reactor efficiency using convex nonlinear optimization as the objective function for the validated mathematical model.

The stoichiometric reaction and kinetics parameters in the simplified biofilm growth model [16] that are considered in the optimization include the maximum consumption rates, half-rate Monod kinetic constants, maximum growth rates, and decay rates. Microorganisms such as fermentative bacteria, acetoclastic methanogenic bacteria, electroactive bacteria, and hydrogenotrophic methanogenic bacteria are assumed to be present in the biofilm system. The maximum attainable biomass concentration on the biofilm was defined for the outer anodic layer, the inner anodic layer, and the cathodic layer.

The bioelectrochemical balance parameters considered in the optimization included current density, applied potential, counter electromotive force for the MEC, maximum resistance, minimum resistance, curve steepness constant, cathode efficiency, and yield rate for the hydrogenotrophic methanogenic bacteria.

Levenberg-Marquardt (LM) is a preferred training algorithm, although it requires more memory than the other options, as reported in the previous ANN modeling study of the biohydrogen fermentation process [21, 22]. Therefore, the LM algorithm was used in the iterative ANN data training to identify the optimal nodes for the single hidden layer. The topology consists of three input nodes (catholyte pH, current density, and applied potential) and one output node (hydrogen production rate).

The use of experimental data is focused on validating the simulation results of the simplified microbial biofilm growth model. The process domains of MEC considered in this study are as follows: (i) a double chamber reactor configuration with a proton exchange membrane as the hydrogen-proton junction; (ii) using as substrate a wastewater sample from a local sago processing mill in Mukah, Sarawak, Malaysia; and (iii) the applied potential ($E_{applied}$) in the range of 0.1 to 0.8 V [1, 23, 24]. The bioelectrochemical efficiencies such as COD removal efficiency, coulombic efficiency, and energy efficiency [25] were used to evaluate the process limit of the model MEC.

2.0 METHODOLOGY

2.1 Source of Experimental Data

In the mathematical modeling study, the experimental data are needed to improve the reliability and validity of the results before they can be used to optimize the MEC process. The data were obtained from the results of a MEC experiment. Briefly, a laboratory-scale dual-chamber MEC was developed consisting of a proton exchange membrane made of pretreated ALDRICH

Nafion 117 in a PVC pipe as a connection between two units of a 4-liter acrylic chamber. Each chamber was equipped with an electrode made of a 0.098 m^2 carbon fiber plate, and the distance between the anode in the anodic chamber and the cathode in the cathodic chamber was set at 11.8 cm. A current source of 1.5 V which has to be higher than the theoretical range between 0.1 to 0.8 V with parallel connection to a fixed resistor of 1,000 Ω connecting the anode to the cathode to form a complete external circuit.

The anodic chamber was filled with anolyte or decanted sago wastewater taken from the effluent of a local sago mill in Mukah, Sarawak, Malaysia. From the pre-analysis, the chemical oxygen demand (COD) was 476 mg·L^{-1} in the influent and 2,430.22 mg·L^{-1} in the anodic chamber based on the readings of HACH DR900, which also indicates the substrate concentration. Meanwhile, the cathodic chamber was filled with catholyte or distilled water, and the pH value of the electrode-based Hanna Instruments pH meter indicated the hydrogen production rate. The microbial reaction in the MEC was left at a pressure of 1 atm and a temperature of 25 °C for 16 retention days, as shown in Figure 1.

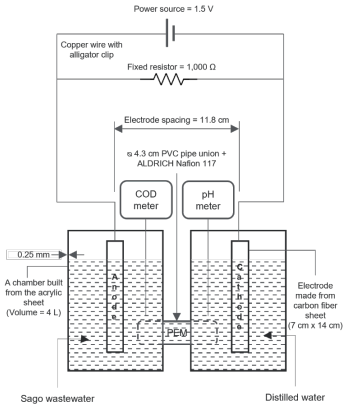

Figure 1 The MEC experimental setup

2.2 Data Training

Hydrogen gas production in the MEC experiment was indicated by the drop in the pH of the distilled water within 16 days of a startup using the electrode-based Hanna Instruments pH meter. However, to the best of the authors' knowledge, there is no formulation for converting pH data into hydrogen production rate units. Therefore, the experimental data for the relationship between catholyte pH, hydrogen production rate in L·day^{-1}, applied potential ($E_{applied}$) in V, and current density (I_0) in A·m^{-2} [20] were used in the ANN training to generate their data-driven equation. The data were randomly divided into 75% for training, 15% for testing, and 15% for validation.

The best-generated matrices or values of the minimum of the normalized output variable data ($Data_{output,\ min}^*$), the offset values between the input layer and the hidden layer ($OS_{I\text{-}H}$), the offset values between the hidden layer and the output layer ($OS_{H\text{-}O}$), the weighting values between the input layer and the hidden layer ($W_{I\text{-}H}$), the weighting values between the hidden layer and the output layer ($W_{H\text{-}O}$), the bias values between the input layer and the hidden layer ($b_{I\text{-}H}$), the bias values between the hidden layer and the output layer ($b_{H\text{-}O}$), the gain values between the input layer and the hidden layer ($g_{I\text{-}H}$), and the gain values between the hidden layer and the output layer ($g_{H\text{-}O}$) were stored to define sigmoid transfer function equation and incorporate the best-trained ANN function into the existing mathematical model.

A total of three input variables, consisting of the experimental values in [12×3] matrices, were included to define normalized input variable data 1 ($Data_{input,1}^*$) for the pH of the catholyte, the normalized input variable data 2 ($Data_{input,2}^*$) for the current density (I_0), and normalized input variable data 3 ($Data_{input,3}^*$) for the applied potential ($E_{applied}$). The pH of the catholyte has a minimum value of 5 and a maximum value of 9, the current density (I_0) has a minimum value of 0.7 A·m^{-2} and a maximum value of 1.9 A·m^{-2}, the applied potential ($E_{applied}$) has a minimum value of 0.6 V and a maximum value of 0.85 V, and the hydrogen production rate has a minimum value of 0.003 L·day^{-1} and a maximum value of 0.066 L·day^{-1} [20]. The normalized output variable data generate the [12×1] matrices of the experimental values of hydrogen production rate in L·day^{-1}.

2.3 Data Normalization

Normalizing the scale data (Data → $Data^*$) and vice versa ($Data^*$ → Data) using equation 1 could eliminate the inaccuracy of data during data training and also the comparison of variable data between modeling and experiment. $Data^*_{min}$ and $Data^*_{max}$ are the constant normalization values, which depend on the requirements of the procedure. Before modeling ANN, $Data^*_{min}$ = 0.1 and $Data^*_{max}$ = 0.8, while the output data of modeling hydrogen production rate should be normalized within the experimental range between $Data^*_{min}$ = 0.003 L·day^{-1} and $Data^*_{max}$ = 0.066 L·day^{-1}.

$$Data^* = \frac{(Data^*_{max} - Data^*_{min})(Data - Data_{min})}{(Data_{max} - Data_{min})} + (Data^*_{min}) \quad (1)$$

2.4 Mathematical Model

The assumptions of the mathematical model follow the conditions of the MEC experiment as follows:

i. A proton exchange membrane in a two-chamber MEC transports the free protons at the anolyte into the catholyte without significant methane formation.

ii. Pure hydrogen is produced at the cathode, but not to the extent that it contributes to significant growth of hydrogenotrophic methanogenic bacteria.

iii. The electrode spacing is optimal for the anode area of the bound electron transferred from the electroactive bacteria, so ohmic losses are relatively low due to the inevitable resistance that protects the current in the circuit from overflowing.

iv. The large diffusion of hydrogen gas at the cathode with an efficiency of 95% resulted in Butler-Volmer losses.

v. The input voltage of 1.5 V is practically an external voltage for the MEC experiment to overcome the non-spontaneous biological reaction at equilibrium electrode potential, since it is usually larger than the theoretical value, such as the average range of MEC, which is between 0.1 and 0.8 V.

vi. The remaining assumptions which are not mentioned or subjected to the changes follow the reference in the literature [16].

The kinetic mechanisms of microbial reaction in three biofilm growth layers system are proposed in Table 1. To summarize, the reaction started with the decomposition of the substrate by the metabolizing fermentative bacteria. The electroactive bacteria mainly consumed the acetate produced to provide the electrons and hydrogen protons. At the same time, the small remainder was converted to methane as a by-product in the presence of acetoclastic methanogenic bacteria [16]. The cathodic chamber also makes no exception for methane formation due to the growth of hydrogenotrophic methanogenic bacteria when the hydrogen produced at the cathode electrode is excessive.

According to the biofilm reaction kinetics, a mathematical model with a total of eight ODEs represents the mass balance of the biofilm communities with respect to their concentration during the reaction over time (e.g., Equation 2 defines the mass balance of substrate concentration). The subscript λ = S, A, f, m1, m2, e, M, and h represents the identity of the specific biofilm community, listed sequentially as follows: Substrate, Acetate, Fermentative, Acetoclastic methanogenic 1, Acetoclastic methanogenic 2, Electroactive, Mediator, and Hydrogenotrophic methanogenic.

Table 1 Kinetic mechanism for the multiple microbial biofilm growth systems [16]

Biofilm layer (k)	Stoichiometric reaction equations
Anodic Outer (k=1): α_1, $X_{max,1}$	Fermentative (f): $C_6H_{12}O_6 \xrightarrow[K_{d,f}]{K_{S,f},q_{max,f},\mu_{max,f}} 3C_2H_4O_2$
	Acetoclastic methanogenic (m,1): $C_2H_4O_2 \xrightarrow[K_{d,m}]{K_{A,m},q_{max,m},\mu_{max,m}} CH_4 + CO_2$
Inner (k=2): α_2, $X_{max,2}$	Acetoclastic methanogenic (m,2): $C_2H_4O_2 \xrightarrow[K_{d,m}]{K_{A,m},q_{max,m},\mu_{max,m}} CH_4 + CO_2$
	Electroactive (e): $C_2H_4O_2 + H_2O + 4M_{ox} \xrightarrow[K_{d,e}]{K_M,K_{A,e},q_{max,e},\mu_{max,e}} 4M_{red} + CO_2$
	$4M_{red} \xrightarrow[K_{d,e}]{K_M,K_{A,e},q_{max,e},\mu_{max,e}} 4M_{ox} + 8e^- + 8H^+$
Cathodic (k=3): α_3, $X_{max,3}$	Hydrogenotrophic methanogenic (h): $CO_2 + 4H_2 \xrightarrow[K_{d,h}]{\mu_{max,h}} CH_4 + 2H_2O$

Note: Substrate = $C_6H_{12}O_6$; Acetate = $C_2H_4O_2$

For the stoichiometric reaction and kinetic parameters, $q_{max,\lambda}$ is the maximum consumption rate of substrate or acetate, $\mu_{max,\lambda}$ is the maximum microbial growth rate, K_λ is the Monod kinetic constant, and $K_{d,\lambda}$ is the microbial decay rate. Electroactive bacteria facilitate the intracellular electron transfer mechanism from the anodic biofilm to the anode surface. Each bacterium that was paired with was limited by the different values of the retention constant α_k and the minimum attainable biomass concentration $X_{max,k}$ in the respective biofilm layer of k, where k = 1 is the outer anodic layer, k = 2 is the inner anodic layer, and k = 3 is the cathodic layer. The value α_k, which is not zero, depends on the sum of the concentration of mating bacteria, which is higher than $X_{max,k}$.

$$\frac{dS}{dt} = -\left(q_{max,f}\frac{S}{K_{S,f}+S}\right)x_f + D(S_0 - S) \quad (2)$$

The constant parameters required in the bioelectrochemical balance are the ideal gas constant of R = 8.31446 mL·atm·L^{-1}·mol^{-1}, Faraday constant of F = 96485 A·s·mole^{-1}, and reduction or oxidation transfer coefficient of β = 0.5. The nonlinear curve of the MEC current was initialized with a steepness constant of K_R = 0.024 L·mg^{-1}. For a double chamber MEC, only hydrogen production rate was quantified using equation 3.

$$Q_{H_2} = Y_{H_2}\left(\frac{I_{MEC}}{mF}\frac{RT}{P}\right) - Y_h\mu_h x_h V \quad (3)$$

The performance of the MEC reactor can be evaluated using the existing model based on the initial values of equation 4 for the removal efficiency of COD ($\eta_{CODremoval}$), equation 5 for the Coulombic efficiency (η_C), and equation 6 for the energy efficiency (η_{EL}) [25]. The initial COD which is constant at 476 mg·L^{-1} minus the final COD also has the same meaning as the differences in substrate concentration over 20 days of time steps, in which the values can be obtained from the recorded data of the ODE graph. As high-efficiency electric energy is required to form the cathodic hydrogen, the cathodic recovery (r_{cat}) can be as high as 100%. The enthalpy changes of the hydrogen reaction, ΔH_2, were equal to 285.83 kJ·mol^{-1} for the standard.

$$\eta_{CODremoved} = \frac{COD_{initial} - COD_{final}}{COD_{initial}} \times 100 \quad (4)$$

$$\eta_C = \frac{8\, I_{MEC}\, t}{V\, F\left(COD_{initial} - COD_{final}\right)} \quad (5)$$

$$\eta_{EL} = \frac{4\, \Delta H_{H_2}\, I_{MEC}\, t\, r_{cat}}{\eta_C\, E_{applied}\, m\, F^2} \quad (6)$$

2.5 Problem Formulation and Optimization Procedure

The optimization goal is to minimize the mean squared error (MSE) between the predicted and experimental values. MSE is more accurate than other statistical parameters, which improved the predictability of the model for the comparative study of multivariate dynamic analysis of fermentative biohydrogen. The $q_{max,f}$, $q_{max,m}$, $q_{max,e}$, $\mu_{max,f}$, $\mu_{max,m}$, $\mu_{max,e}$, $\mu_{max,h}$, $K_{S,f}$, $K_{A,m}$, $K_{A,e}$, K_M, $K_{d,f}$, $K_{d,m}$, $K_{d,e}$, $K_{d,h}$, $X_{max,1}$, $X_{max,2}$, and $X_{max,3}$, which refer to the stoichiometric reaction and kinetic parameters, are considered as the decision variables for optimization in the substrate concentration profile problem, which can be expressed in equation 7:

$$\text{Minimize} \quad MSE = \frac{\sum_{i=1}^{N}(S_{exp} - S_{pred})^2}{N} \quad (7)$$

Subject to the constraints:

$q_{max,f} \geq 0$ mg·mg^{-1}·day^{-1}

6.00 mg·mg^{-1}·day^{-1} ≤ $q_{max,m}$ ≤ 14.12 mg·mg^{-1}·day^{-1}

14 mg·mg^{-1}·day^{-1} ≤ $q_{max,e}$ ≤ 500 mg·mg^{-1}·day^{-1}

0 day^{-1} ≤ $\mu_{max,f}$ ≤ 25 day^{-1}

0.1 day^{-1} ≤ $\mu_{max,m}$ ≤ 4.0 day^{-1}

1.97 day^{-1} ≤ $\mu_{max,e}$ ≤ 8.00 day^{-1}

$0.35\ day^{-1} \le \mu_{max,h} \le 0.48\ day^{-1}$
$375\ mg \cdot L^{-1} \le K_{S,f} \le 400{,}000\ mg \cdot L^{-1}$
$1\ mg \cdot L^{-1} \le K_{A,m} \le 80\ mg \cdot L^{-1}$
$19\ mg \cdot L^{-1} \le K_{A,e} \le 21\ mg \cdot L^{-1}$
$0\ mg \cdot L^{-1} \le K_M \le 20.0\ mg \cdot L^{-1}$
$0.004\ day^{-1} \le K_{d,f} \le 8.000\ day^{-1}$
$0.000\ day^{-1} \le K_{d,m} \le 0.002\ day^{-1}$
$0.0000\ day^{-1} \le K_{d,e} \le 0.0394\ day^{-1}$
$0.01\ day^{-1} \le K_{d,h} \le 0.11\ day^{-1}$
$80 \le X_{max,1} \le 215$
$512.5 \le X_{max,2} \le 2{,}000.0$
$160 \le X_{max,3} \le 1{,}680$

Meanwhile, I_0, $E_{applied}$, E_{CEF}, R_{max}, R_{min}, K_R, Y_{H2}, and Y_h are the bioelectrochemical balance parameters defined as the decision variables for the hydrogen production rate profile problem, as in equation 8.

$$\text{Minimize} \quad MSE = \frac{\sum_{i=1}^{N} (Q_{H_2,exp} - Q_{H_2,pred})^2}{N} \tag{8}$$

Subject to the constraints:
$0.7\ A \cdot m^{-2} \le I_0 \le 1.9\ A \cdot m^{-2}$
$0.1\ V \le E_{applied} \le 0.8\ V$
$-0.9\ V \le E_{CEF} \le 0.0\ V$
$25 \le R_{max} \le 2{,}000\ \Omega$
$0\ \Omega \le R_{min} \le 25\ \Omega$
$0\ L \cdot mg^{-1} \le K_R \le 1\ L \cdot mg^{-1}$
$0 \le Y_{H2} \le 1$
$1{,}500\ mL \cdot mg^{-1} \le Y_h \le 7{,}000\ mL \cdot mg^{-1}$

As the objectives are nonlinear, solving the problems based on the convex optimization routine helps obtain a feasible solution that satisfies the objectives. The constraints in formulating the optimization problem were set by repeatedly manipulating the input values of the decision variables, one by one, to find the profile with the lowest MSE. All decision variables must lie within the lower and upper bounds to achieve the optimum. Convex optimization was performed by calling the ODEs function into a nonlinear optimization routine solved by the minimization constraint function. Finally, the search focused on finding the mean or low uncertainty range (if any) of the model input parameters that could minimize the percent gap between the modeling data and the experimental data for the substrate profile and the hydrogen production rate profile at any time step.

The validated model was then extended for process limitation analysis by maximizing the percent MEC efficiency of COD removal ($\eta_{CODremoval}$), Coulombic (η_C), and energy (η_{EL}) according to equation 9 with respect to the decision variables $E_{applied}$, $A_{surf,anode}$, V, and S_0.

$$\text{Maximize} \quad \begin{cases} f(\eta_{CODremoved}) = -\eta_{CODremoved} + \dfrac{COD_{initial} - COD_{final}}{COD_{initial}} \times 100 \\ f(\eta_C) = -\eta_C + \dfrac{8\, I_{MEC}\, t}{V F (COD_{initial} - COD_{final})} \\ f(\eta_{EL}) = -\eta_{EL} + \dfrac{4\, \Delta H_{H_2}\, I_{MEC}\, t\, r_{cat}}{\eta_C\, E_{applied}\, m F^2} \end{cases} \tag{9}$$

Subject to the constraints:
$0.1\ V \le E_{applied} \le 0.8\ V$
$0.02\ m^2 \le A_{surf,anode} \le 0.10\ m^2$
$3\ L \le V \le 10\ L$
$1{,}500\ mg \cdot L^{-1} \le S_0 \le 7{,}000\ mg \cdot L^{-1}$
$0\% \le \eta_{CODremoval} \le 100\%$
$0\% \le \eta_C \le 100\%$
$0\% \le \eta_{EL} \le 100\%$

3.0 RESULTS AND DISCUSSION

3.1 Experimental Validation of the Mathematical Model

The proposed methodology of modeling and optimization was performed using MATLAB (R2022a software license number: 40774331). The solver ode45 was chosen to calculate the output of the ODEs of the model as interpolation of the data within the time step could provide a more uniform solution. As data collection from the retention time experiment lasted up to 16 days, the mathematical modeling period was extended to a maximum of 20 days to ensure that the profiles from ODE reached a steady state.

3.1.1 Substrate Concentration Profile

The state variables and the stoichiometric reaction and kinetics parameters of the mathematical model were initialized with the input values proposed in the literature [16, 26]. The substrate concentration curve was generated using only the data from Yahya et al. [26] with the exception of the substrate concentration at the initial state ($S_{t=0}$) equal to $2{,}430.22\ mg \cdot L^{-1}$ follows the conditions of the experiment. Replacing the literature value of the substrate concentration in the influent (S_i) with the experiment condition, from 2,000 to 476 $mg.L^{-1}$ resulting to a slightly decreased of the discrepancy of the initial curve with the experimental data (see in Figure 2).

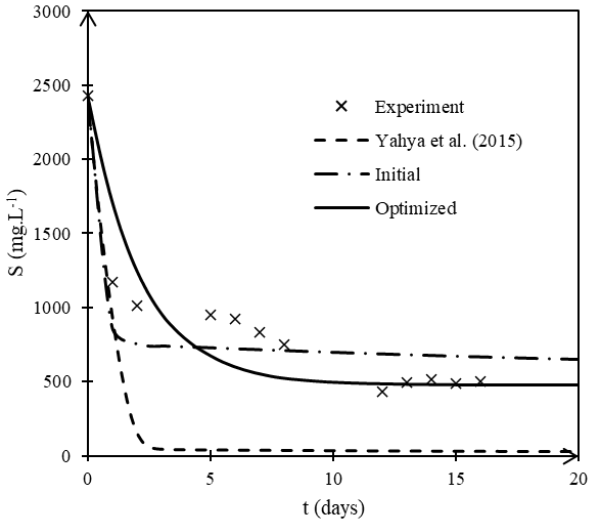

Figure 2 Comparison of the substrate concentration profile

The poor simulation results due to the relatively large MSE of the initial curve were effectively minimized with the subsequent optimization step of the model based on the convex method using the minimization constraint function of the solver. The initial conditions of the eight state variables (S, A, x_f, x_{m1}, x_e, x_{m2}, x_h, M_{ox}) of the ODEs in the model were first defined using the literature data [16, 26] before they were finally adjusted to the

optimal values, where the initial concentration of acetate of $A_{t=0}$ = 0.786 mg·L^{-1}, fermentative bacteria of $x_{f(t=0)}$ = 61.0 mg·L^{-1}, acetoclastic methanogenic bacteria of $x_{m1(t=0)}$ = $x_{m2(t=0)}$ = 43.5 mg·L^{-1}, electroactive bacteria of $x_{e(t=0)}$ = 21.0 mg·L^{-1}, hydrogenotrophic methanogenic bacteria of $x_{h(t=0)}$ = 70.0 mg·L^{-1}, and oxidized mediator of $M_{ox(t=0)}$ = 0.285%.

These initial values of state variables indicate that the stored energy (i.e., the carbohydrates in the sago effluent) [15, 27, 28] is not sufficient for the fermentative bacteria to spontaneously degrade the complex carbon of the substrate into a simple structure, such as acetate [5] as the primary source of free electrons and hydrogen protons due to the significant positive Gibbs free energy of the endothermic reactions [1]. Microbial conversion does not begin until a small external energy greater than the equilibrium electrode potential, identified as E_{CEF} = -0.16 V, is added to the MEC circuit to allow the formation of hydrogen gas at the cathode by reduction and oxidation (redox) [3–5].

Prior to optimization, the influence of the stoichiometric reaction and kinetics parameters on the minimum steady state substrate concentration was analysed using a sensitivity study by manipulating the input value of one variable within ±75% of its initial value while holding the others constant. The range of input values for each parameter that resulted in the changes in the overall substrate concentration curve over time was used to define the lower and upper bounds as the constraints of the minimize function problem. The predictability of the model was significantly improved, as shown by the shift of the initial curve toward the concentrated region of the experimental data covered by the optimized curve corresponding to the best input values for each parameter (see Table 2).

Table 2 The input values of the stoichiometric reaction and kinetic model

Parameters	Yahya et al. [26]	Initial	Optimized	Units
S_i	2,000	476	476	mg·L^{-1}
A_i	1,000	1,000	1,000	mg·L^{-1}
$S_{(t=0)}$	2,430.22	2,430.22	2,430.22	mg·L^{-1}
$A_{t=0}$	0	0	0.786	mg·L^{-1}
$x_{f(t=0)}$	50	50	61.0	mg·L^{-1}
$x_{m1(t=0)}$	50	50	43.5	mg·L^{-1}
$x_{m2(t=0)}$	1	1	43.5	mg·L^{-1}
$x_{e(t=0)}$	50	50	21.0	mg·L^{-1}
$x_{h(t=0)}$	10	10	70.0	mg·L^{-1}
$M_{ox(t=0)}$	0	0	0.285	%
$q_{max,f}$	16.28	16.28	0.00	mg·mg^{-1}·day^{-1}
$q_{max,m}$	14.12	14.12	7.42	mg·mg^{-1}·day^{-1}
$q_{max,e}$	14	14	15	mg·mg^{-1}·day^{-1}
$K_{S,f}$	250	250	376	mg·L^{-1}
$K_{A,m}$	80.0	80.0	1.4	mg·L^{-1}
$K_{A,e}$	20.0	20.0	19.6	mg·L^{-1}
K_M	0.001	0.001	0.000	mg·L^{-1}
$\mu_{max,f}$	0.2	0.2	0.0	day^{-1}
$\mu_{max,m}$	0.1	0.1	1.0	day^{-1}
$\mu_{max,e}$	1.97	1.97	3.30	day^{-1}
$\mu_{max,h}$	0.45	0.45	0.40	day^{-1}
$K_{d,f}$	0.004	0.004	0.954	day^{-1}
$K_{d,m}$	0.002	0.002	0.000	day^{-1}
$K_{d,e}$	0.039	0.039	0.000	day^{-1}
$K_{d,h}$	0.01	0.01	0.06	day^{-1}
$X_{max,1}$	900	900	81	
$X_{max,2}$	513	513	514	
$X_{max,3}$	1,680	1,680	161	

It was found that the electroactive bacteria for acetate consumption rate ($q_{max,e}$) and half-rate Monod constant ($K_{A,e}$), the hydrogenotrophic methanogenic bacteria for growth rate ($\mu_{max,h}$) and decay rate ($K_{d,h}$), and the maximum attainable biomass concentration at the inner anodic biofilm layer ($X_{max,2}$) for the sago effluent are within the range of reaction rates or constant with the average organic wastewater, as indicated by a slight deviation of the optimized values compared to the initial values.

The optimized nonlinear curve of the model overestimates and underestimates the substrate concentration for the undershoot data at a time between 1 and 2 days and the overshoot data at a time between 5 and 8 days, which can be attributed to the negligible dynamic effect of the uncertainty parameters or the reaction and kinetic rates in the analysis of the experiment over 16 days retention time. This could be related to the strong influences of the multivariate input factors, such as the minimum steady state of the substrate concentration curve that is decreased with a decrease in the substrate consumption rates of the fermentative bacteria ($q_{max,f}$), the half-rate of the kinetic Monod of the fermentative bacteria ($K_{S,f}$), but with the increase in the acetate consumption rates of the electroactive bacteria ($q_{max,e}$), the decay rates of the fermentative bacteria ($K_{d,f}$), and the decrease and increase in the growth rates of the acetoclastic methanogenic bacteria ($\mu_{max,m}$). Meanwhile the other input factors in the stoichiometric reaction and kinetics model are characterized as constant parameters, which is reflected in the small percentage changes in the minimum steady state substrate concentration in Table 3.

Table 3 The sensitivity of the stoichiometric reaction and kinetics factors to the minimum steady-state substrate concentration

Variation (%)	-75	0	+75
Parameters	Changes in the minimum steady-state substrate concentration (%)		
$q_{max,f}$	-0.016	0.000	0.001
$q_{max,m}$	0.003	0.000	0.001
$q_{max,e}$	-0.005	0.000	-0.018
$K_{S,f}$	-0.012	0.000	0.000
$K_{A,m}$	-0.007	0.000	0.003
$K_{A,e}$	-0.001	0.000	-0.005
K_M	0.000	0.000	0.004
$\mu_{max,f}$	-0.001	0.000	-0.006
$\mu_{max,m}$	-0.012	0.000	-0.019
$\mu_{max,e}$	0.001	0.000	-0.001
$\mu_{max,h}$	-0.006	0.000	-0.008
$K_{d,f}$	0.002	0.000	-0.017
$K_{d,m}$	-0.001	0.000	0.005
$K_{d,e}$	-0.005	0.000	-0.005
$K_{d,h}$	-0.003	0.000	0.001
$X_{max,1}$	0.000	0.000	-0.005
$X_{max,2}$	0.001	0.000	-0.006
$X_{max,3}$	-0.006	0.000	-0.003

3.1.2 Hydrogen Production Rate Profile

Prior to experimental validation of the hydrogen production rate model, the output value of the hydrogen production rate corresponding to the input value of the pH of the catholyte was calculated directly using Sigmoid transfer function, which consists of stored matrices or values of the best weights, biases,

gains, and offsets at a constant input value of the current density of I_0 = 0.632 A·m^{-2} and an applied potential of $E_{applied}$ = 0.8 V. The data training was carried out on the experimental hydrogen production rate. The best data training based on the Levenberg-Marquardt algorithm was achieved for the optimal neurons for a single hidden layer of 10, as shown by the resulting MSE of 0.00625 and the coefficient of determination (R-squared) of 1 for the sigmoid transfer function of the topology with three layers between three input neurons (pH of the catholyte, I_0, $E_{applied}$) and one output neuron (hydrogen production rate).

Each hydrogen production rate profile curve in Figure 3 was generated using the same input values of the eight state variables, stoichiometric reaction and kinetics parameters for the respective substrate concentration profile curve as previously discussed, but this time with the inclusion of the bioelectrochemical balance in the model consisting of the input values of the varied parameters as recorded in Table 4. Using the input data from the literature [16, 26], the overall profile of the hydrogen production rate showed a significant discrepancy with the experimental data. The nonlinearity of the experimental data caused the model to overestimate the hydrogen production rate for the undershoot data in a period between 0 and 16 days.

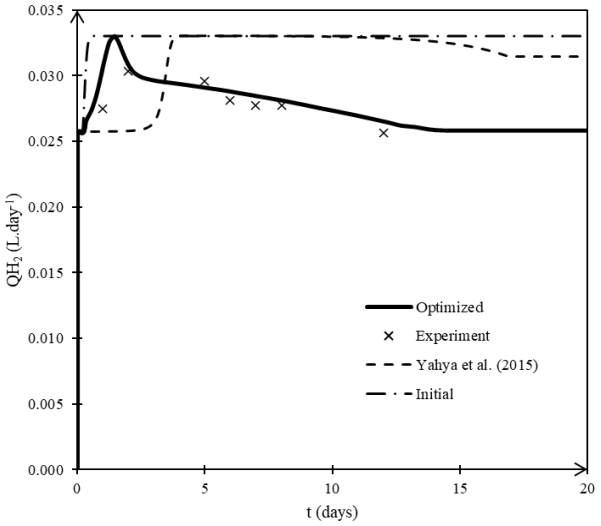

Figure 3 Comparison of the hydrogen production rate profile

Table 4 The input values of the bioelectrochemical balance parameters

Parameters	Yahya et al. [26]	Initial	Optimized	Units
I_0	0.006	0.006	0.632	A·m^{-2}
$E_{applied}$	10.0	10.0	0.8	V
E_{CEF}	-0.34	-0.34	-0.16	V
R_{max}	2,000	2,000	1,000	Ω
R_{min}	25	25	0	Ω
K_R	0.024	0.024	0.491	L·mg^{-1}
Y_{H2}	0.90	0.90	0.95	
Y_h	0.00005	0.00005	0.00816	mL·mg^{-1}

The rapid increase in hydrogen production rate to the peak value of 0.033 L·day^{-1} at a time less than 1.64 days was overestimated by the model before optimization was performed. The curve of Yahya et al. [26], which remains constant at the initial value of 0.0257 L·day^{-1}, is due to the fact that some input parameters of the stoichiometric reaction and kinetics are not within the experimental range. When the initial substrate concentration in the influent (S_i) follows the experimental condition, the model responds with a rapid increase to a maximum steady state of 0.033 L·day^{-1}, which describes a strong dynamic correlation between the substrate and hydrogen production.

The steady state curve of Yahya et al. [26] at 0.0257 L·day^{-1} as well as the initial curve at 0.033 L·day^{-1} showed an argument of the model assuming a rapid decline after the peak value of 0.033 L·day^{-1} was reached at a time between 1.64 and 2 days, which was due to the overvoltage difference of the applied potential ($E_{applied}$) between the literature [26] and the MEC experimental setup.

The gradual decrease in hydrogen production rate to the steady state of 0.026 L·day^{-1} in a period between 2 and 13.76 days in the experiment showed the opposite effect in the modeling as a significant increase to the maximum steady state of 0.066 L·day^{-1} when Yahya et al. [26] proposed substrate concentration in the influent (S_i) does not correspond to the experimental conditions, but indicates the curve for the initial steady state of 0.033 L·day^{-1}, which could be due to the values of some factors in the bioelectrochemical balance reported in the literature that are not within the desired range for the experimental conditions.

The results of curve fitting of the model together with minimization of the MSE with respect to the input values of the bioelectrochemical balance factors showed that the optimized curve of hydrogen production rate curve covers the concentration range of the experimental data. The ignorance of the nonlinear interaction in the experiment for the factors involved in the stoichiometric reaction and kinetic and bioelectrochemical balance caused the optimized model to underestimate the hydrogen production rate for the overshoot data at a time of 5 days. This could be due to the decrease in all bioelectrochemical parameters in Table 5, except for the maximum resistance (R_{max}) and the curve steepness constant (K_R), and conversely, the increase effect that caused the model to overestimate the undershoot data at a time between 1 and 2 days and between 6 and 12 days. It was also noticeable that the applied potential ($E_{applied}$) was the largest contributor to the significant effect on the steady state hydrogen production rate, followed by the minimum resistance (R_{min}), cathodic efficiency (Y_{H2}), and counter electromotive force potential (E_{CEF}).

Table 5 The sensitivity of the bioelectrochemical balance factors on the steady state hydrogen production rate

Variation (%)	-75	0	+75
Parameters	Changes in the steady state hydrogen production rate (%)		
I_0	-19.01	0.00	-4.77
$E_{applied}$	-1342.89	0.00	-1343.68
E_{CEF}	-42.71	0.00	-43.27
R_{max}	0.00	0.00	0.00
R_{min}	-303.32	0.00	42.44
K_R	0.00	0.00	0.00
Y_{H2}	72.08	0.00	-75.50
Y_h	-0.83	0.00	-0.73

3.2 Process Limits

The optimized substrate concentration and hydrogen production rate results improved the validity of the mathematical model used as a benchmark for the sensitivity study of the effects of MEC operating keys on bioelectrochemical process performance. The applied potential ($E_{applied}$), anode surface area ($A_{surf,anode}$), anodic compartment volume (V), and initial substrate concentration (S_0) are the four manipulated variables that were subjected to the influences of the maximum steady-state percentage of three efficiency categories, including COD removal ($\eta_{CODremoval}$), Coulombic (η_C), and energy (η_{EL}). Benchmark values were determined from the confirmed model as follows: $E_{applied}$ = 0.8 V, $A_{surf,anode}$ = 0.098 m^2, V = 4 L, and S_0 = 2,430.22 mg·L^{-1}.

3.2.1 MEC Efficiency Evaluation

The variation of the applied potential ($E_{applied}$) at 0.1 V gaps in Figure 4, while the other manipulated parameters were kept constant, where $A_{surf,anode}$ = 0.098 m^2, V = 4 L, and S_0 = 2,430.22 mg·L^{-1} showed that the coulombic efficiency has a significant effect only above 0.7 V due to single effect manipulation. The model considered as the allowable range for the oxidation of the organic compounds of the sago wastewater without current losses during electron transfer [16]. At the same time, the energy efficiency decreased exponentially with the increase of the applied potential from 0.1 to 0.8 V, which is the average range required by the MEC to produce the same amount of hydrogen as in water splitting [1], due to the desirable high bioelectrochemical conversion of sago wastewater substrate to hydrogen at a very low external input voltage to the electrode circuit.

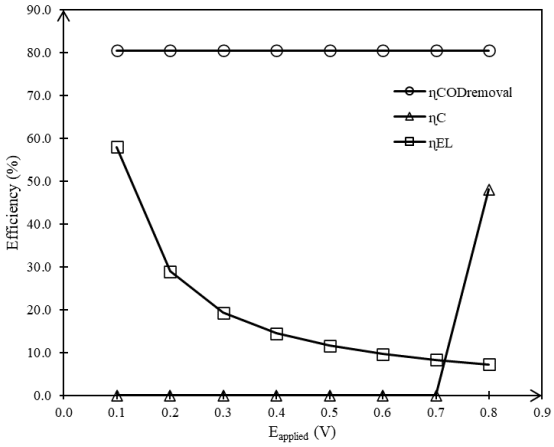

Figure 4 The influences of MEC efficiency by varying applied potential

Figure 5 shows the variation of the anode surface area ($A_{surf,anode}$) at a change step of 0.02 m^2, while the other manipulated parameters were kept constant, $E_{applied}$ = 0.8 V, V = 4 L, and S_0 = 2,430.22 mg·L^{-1} demonstrates the increase in Coulombic efficiency with the increase in anode surface area between 0.02 and 0.05 m^2 and between 0.06 and 0.10 m^2, which can be explained by the fact that with a larger contact area of the anode electrode, more electrons can be transferred to the circuit from the oxidation in the anodic biofilm.

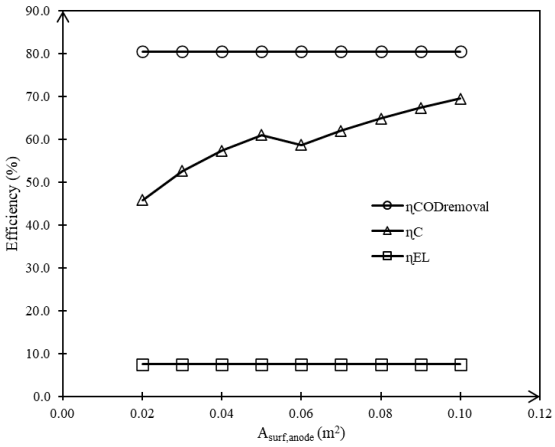

Figure 5 The influences of MEC efficiency by varying anode surface area

The volume of the anodic compartment was varied in Figure 6 at 1 L difference up to the maximum of 10 L [26], while the other manipulated parameters were kept constant: $E_{applied}$ = 0.8 V, $A_{surf,anode}$ = 0.098 m^2, and S_0 = 2,430.22 mg·L^{-1}. The first observation was that the Coulombic efficiency (η_C) decreased linearly with the increase of the volume of the anodic chamber, because the use of sago wastewater is more efficient when it is placed in a small chamber with anode electrode to oxidize the chemical energy stored in the organic compound into electrical energy in the external circuit after the anode electrode accepts free electrons. The second observation was the energy efficiency (η_{EL}), which increases slightly as the volume of the anode chamber increases because more hydrogen energy can be recovered from the electrically driven redox process with a larger chamber.

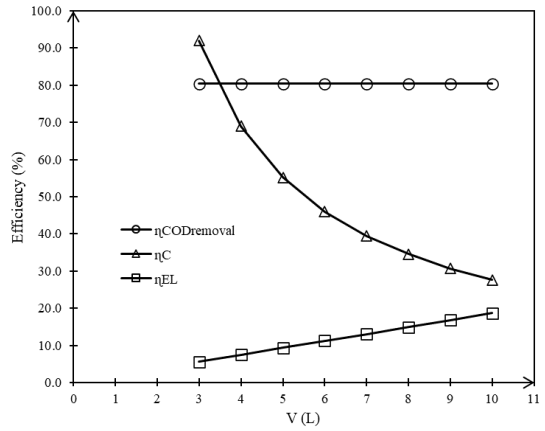

Figure 6 The influences of MEC efficiency by varying anodic volume

The initial substrate concentration in the anode chamber manipulated within 1,000 mg·L^{-1} in Figure 7, while holding the other manipulated parameters values constant, $E_{applied}$ = 0.8 V, $A_{surf,anode}$ = 0.098 m^2, V = 4 L. The first observation was that the initial substrate concentration was the only operating key that showed a significant effect on the COD removal efficiency ($\eta_{CODremoval}$). The slight increase occurred until a maximum steady state was reached. The substrate removal reached the highest efficiency to provide acetate with a broader interface between the distribution of the carbon source in the bulk anodic phase

and the metabolizing anodic bacteria in the anodic biofilm phase. The second observation was the increase in Coulombic efficiency (η_C) to the highest peak of percentage between 2,500 and 3,000 mg·L^{-1} where the sago wastewater substrate reached its highest conversion. The third observation was the steady increase in energy efficiency (η_{EL}) with the increase in initial substrate concentration, as more biohydrogen can be obtained at the cathode when more concentrated sago effluent is fed into the anodic chamber of the MEC. However, the Coulombic efficiency seems to fluctuate with the increase of substrate concentration beyond the highest peak, which means that the MEC model is only effective for processing the fed wastewater up to the maximum allowed concentration of 3,000 mg·L^{-1}.

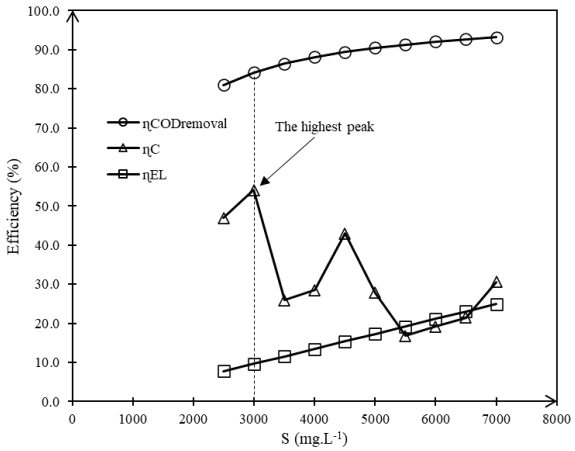

Figure 7 The influences of MEC efficiency by varying initial substrate concentration

3.2.2 Process Optimization

The maximum steady-state percentages of COD removal efficiency ($\eta_{CODremoval}$), Coulombic efficiency (η_C), and energy efficiency (η_{EL}) could be obtained with the identification of the process limits of the MEC or the optimal values of the different input operating keys such as the applied potential ($E_{applied}$), the anode surface area ($A_{surf,anode}$), the volume of the anodic compartment (V), and the initial substrate concentration (S_0). The search was subject to the constraint of the multiple objective function or the upper and lower limits of the input factors corresponding to the same range used in the single effect analysis, such as the applied potential ($E_{applied}$) between 0.1 and 0.8 V, the anode surface area ($A_{surf,anode}$) between 0.02 and 0.10 m^2, the volume of the anodic compartment (V) between 3 and 10 L, and the initial substrate concentration (S_0) between 2,500 and 7,000 mg·L^{-1}.

The model obtained the feasible solution after considering the multiple variation of the input variables where the optimal applied potential is 0.485 V, the anode surface area is 0.098 m^2, the volume of the anodic compartment is 4 L, and the initial substrate concentration is 2,500.99 mg·L^{-1} to achieve the maximum COD removal efficiency of 81.99%, Coulombic efficiency of 69.01%, and energy efficiency of 7.47%.

The optimization, considering the effects of multiple input variables, improved the Coulombic efficiency of the model to a maximum of 69.01% at an applied potential of 0.485 V, which was initially 0% below 0.7 V in the sensitivity analysis for the sole effect of the applied potential on the Coulombic efficiency. This can be attributed to the initial substrate concentration being a significant contributor to the changes in Coulombic efficiency, with the highest peak (69.01%) determined at 2,500.99 mg·L^{-1}.

Moreover, the initial substrate concentration was also the only varying input factor that significantly affected the COD removal efficiency, with an optimal maximum of 81.99% at the concentration (2,500.99 mg·L^{-1}) at which the Coulombic efficiency reached the highest value. The applied potential above 0.45 V ensures that the equilibrium growth of electroactive bacteria in the anodic biofilm could survive until the last day of the process [18], which was consistent with the optimized model (0.485 V) to obtain cathodic hydrogen from MEC at low energy demand.

On the other hand, the optimal anode surface area and volume of the anodic chamber remained at 0.098 m^2 and 4 L, respectively, showing that the model is able to improve MEC efficiency by keeping the same dimensions of the carbon fiber plate (electrode) and the chamber built from acrylic sheets, but only adjusting the initial COD of sago wastewater (initial substrate concentration) from 2,430.22 mg·L^{-1} to 2,500.99 mg·L^{-1} and reduce the input voltage at the external circuit (applied potential) from 0.8 V to 0.485 V.

When the model used the new input of applied potential of 0.485 V, anode surface area of 0.098 m^2, volume of anodic compartment of 4 L, and initial substrate concentration of 2,500.99 mg·L^{-1}, the hydrogen production rate curve in Figure 8 showing an extreme increase until reaching the steady state at a time inferior to 0.54 days, when the oxidation of the substrate is most active, which increases the number of hydrogen protons that can be reduced by electrons at the cathode.

The hydrogen production rate then slowly reached a steady state of 0.033 L·day^{-1} at a time superior to 0.54 days when the availability of the substrate for degradation became more limited and the interface for acetate distribution narrowed, as shown by the linear decrease of the substrate from fast then slow to the steady state of 476.89 mg·L^{-1} at a time inferior to 5 days. This observation proves that the dynamic behaviour of hydrogen production rate strongly depends on the performance of the MEC process, which includes the efficiency of substrate degradation, the efficiency of sago wastewater as substrate, and the efficiency of redox hydrogen recovery.

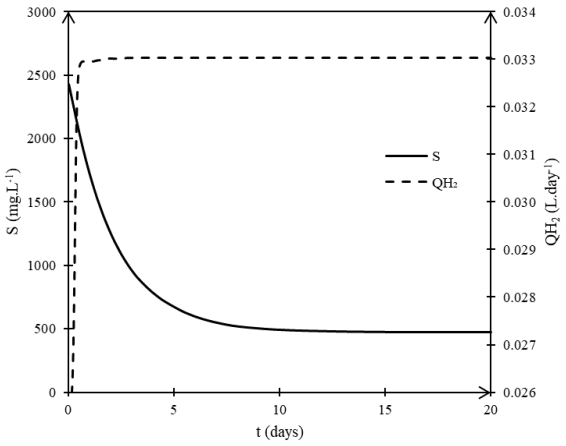

Figure 8 The profile of the output variables of the model under the optimal conditions of the MEC process

4.0 CONCLUSION

Nonlinear convex optimization of the input values of the parameter associated with the stoichiometric reaction and kinetics and bioelectrochemical balance improved the validity of the results of the mathematical model approximating the experimental data of the sago effluent-fed MEC over 16 retention days for the substrate concentration profile and the hydrogen production rate profile. The ANN also proved that the model is able to predict the experimental hydrogen production rate based on the input of the pH of the catholyte at constant applied potential and constant current density. The optimal input values for the operating conditions of applied potential, anode surface area, anodic chamber volume, and initial substrate concentration lead to the maximum percentages of COD removal efficiency, Coulombic efficiency, and energy efficiency of the model MEC, which indirectly improved the profile of hydrogen production rate and substrate concentration over time.

Acknowledgement

The authors would like to acknowledge Osaka Gas Foundation of International Cultural Exchange (OGFICE) Office, Japan for funding this research through Research Grant Scheme (grant numbers INT/F02/OSAKA-IG/85661/2023). Last but not least, the authors would also thank the Universiti Malaysia Sarawak (UNIMAS): Malaysia for providing the facilities to execute this research.

References

[1] Aboelela, D., Soliman, Moustafa, A. and Ashour, I. 2020. A reduced model for microbial electrolysis cells. *International Journal of Innovative Technology and Exploring Engineering*, 9(4): 1724–1730. DOI: https://doi.org/10.35940/ijitee.D1613.029420

[2] Varanasi, J. L., Veerubhotla, R., Pandit, S. and Das, D. 2019. Biohydrogen Production using Microbial Electrolysis Cell. In *Microbial Electrochemical Technology*. 843–869. Elsevier. DOI: https://doi.org/10.1016/B978-0-444-64052-9.00035-2

[3] Hernández-García, K. M., Cercado, B., Rodríguez, F. A., Rivera, F. F. and Rivero, E. P. 2020. Modeling 3D current and potential distribution in a microbial electrolysis cell with augmented anode surface and non-ideal flow pattern. *Biochemical Engineering Journal*, 162: 107714. DOI: https://doi.org/10.1016/j.bej.2020.107714

[4] Hernández-García, K. M., Cercado, B., Rivero, E. P. and Rivera, F. F. 2020. Theoretical and experimental evaluation of the potential-current distribution and the recirculation flow rate effect in the performance of a porous electrode microbial electrolysis cell (MEC). *Fuel*, 279: 118463. DOI: https://doi.org/10.1016/j.fuel.2020.118463

[5] Xing, D., Yang, Y., Li, Z., Cui, H., Ma, D., Cai, X. and Gu, J. 2020. Hydrogen Production from Waste Stream with Microbial Electrolysis Cells. In *Bioelectrosynthesis*. 39–70. Wiley. DOI: https://doi.org/10.1002/9783527343829.ch2

[6] Flores-Estrella, R. A., de Jesús Garza-Rubalcava, U., Haarstrick, A. and Alcaraz-González, V. 2019. A dynamic biofilm model for a microbial electrolysis cell. *Processes*, 7(4): 183. DOI: https://doi.org/10.3390/pr7040183

[7] Hua, T., Li, S., Li, F., Zhou, Q. and Ondon, B. S. 2019. Microbial electrolysis cell as an emerging versatile technology: a review on its potential application, advance and challenge. *Journal of Chemical Technology and Biotechnology*, 94(6): 1697–1711. DOI: https://doi.org/10.1002/jctb.5898

[8] Deaver, J. A., Kerr, C. A. and Popat, S. C. 2022. Primary sludge-based blackwater favors electrical current over methane production in microbial electrochemical cells. *Journal of Water Process Engineering* 47: 102848. DOI: https://doi.org/10.1016/j.jwpe.2022.102848

[9] Sharma, M., Salama, E.-S., Thakur, N., Alghamdi, H., Jeon, B.-H. and Li, X. 2023. Advances in the biomass valorization in bioelectrochemical systems: A sustainable approach for microbial-aided electricity and hydrogen production. *Chemical Engineering Journal*. 465: 142546. DOI: https://doi.org/10.1016/j.cej.2023.142546

[10] Kurniawan, S., Abdullah, S., Imron, M., Said, N., Ismail, N., Hasan, H., Othman, A. and Purwanti, I. 2020. Challenges and opportunities of biocoagulant/bioflocculant application for drinking water and wastewater treatment and its potential for sludge recovery. *International Journal of Environmental Research and Public Health*, 17(24): 9312. DOI: https://doi.org/10.3390/ijerph17249312

[11] Alazaiza, M., Albahnasawi, A., Ali, G., Bashir, M., Nassani, D., Al Maskari, T., Amr, S. and Abujazar, M. 2022. Application of natural coagulants for pharmaceutical removal from water and wastewater: A review. *Water*, 14(2): 140. DOI: https://doi.org/10.3390/w14020140

[12] Anusha, P., Ragavendran, C., Kamaraj, C., Sangeetha, K., Thesai, A. S., Natarajan, D. and Malafaia, G. 2023. Eco-friendly bioremediation of pollutants from contaminated sewage wastewater using special reference bacterial strain of Bacillus cereus SDN1 and their genotoxicological assessment in Allium cepa. *Science of The Total Environment*, 863: 160935. DOI: https://doi.org/10.1016/j.scitotenv.2022.160935

[13] Periyasamy, P. 2021. Estimation of economic loss of agricultural production and livestock population in Tamil Nadu due to sago industrial pollution: A case study. *Grassroots Journal of Natural Resources*, 4(2): 165–178. DOI: https://doi.org/10.33002/nr2581.6853.040212

[14] Alcaraz–Gonzalez, V., Rodriguez–Valenzuela, G., Gomez–Martinez, J. J., Dotto, G. L. and Flores–Estrella, R. A. 2021. Hydrogen production automatic control in continuous microbial electrolysis cells reactors used in wastewater treatment. *Journal of Environmental Management*, 281: 111869. DOI: https://doi.org/10.1016/j.jenvman.2020.111869

[15] Guo, Z. and Yang, C. 2020. Microbial Metabolism Kinetics and Interactions in Bioelectrosynthesis System. In *Bioelectrosynthesis*, pp. 363–394. Wiley. DOI: https://doi.org/10.1002/9783527343829.ch15

[16] Pinto, R. P., Srinivasan, B., Escapa, A. and Tartakovsky, B. 2011. Multi-population model of a microbial electrolysis cell. *Environmental Science and Technology*, 45(11): 5039–5046. DOI: https://doi.org/10.1021/es104268g

[17] Thirugnanasambandham, K. and Shine, K. 2016. Hydrogen gas production from sago industry wastewater using electrochemical reactor: Simulation and validation. *Energy Sources, Part A: Recovery, Utilization, and Environmental Effects*, 38(15): 2258–2264. DOI: https://doi.org/10.1080/15567036.2016.1174755

[18] Flores-Estrella, R. A., Rodríguez-Valenzuela, G., Ramírez-Landeros, J. R., Alcaraz-González, V. and González-Álvarez, V. 2020. A simple microbial electrochemical cell model and dynamic analysis towards control design. *Chemical Engineering Communications*, 207(4): 493–505. DOI: https://doi.org/10.1080/00986445.2019.1605360

[19] Dudley, H. J., Lu, L., Ren, Z. J. and Bortz, D. M. 2019. Sensitivity and bifurcation analysis of a differential-algebraic equation model for a microbial electrolysis cell. *SIAM Journal on Applied Dynamical Systems*, 18(2): 709–728. DOI: https://doi.org/10.1137/18M1172223

[20] Kyazze, G., Popov, A., Dinsdale, R., Esteves, S., Hawkes, F., Premier, G. and Guwy, A. 2010. Influence of catholyte pH and temperature on hydrogen production from acetate using a two chamber concentric tubular microbial electrolysis cell. *International Journal of Hydrogen Energy*, 35(15): 7716–7722. DOI: https://doi.org/10.1016/j.ijhydene.2010.05.036

[21] Hosseinzadeh, A., Zhou, J. L., Altaee, A., Baziar, M. and Li, D. 2020. Effective modelling of hydrogen and energy recovery in microbial electrolysis cell by artificial neural network and adaptive network-based fuzzy inference system. *Bioresource Technology*, 316: 123967. DOI: https://doi.org/10.1016/j.biortech.2020.123967

[22] Wang, Y., Yang, G., Sage, V., Xu, J., Sun, G., He, J. and Sun, Y. 2021. Optimization of dark fermentation for biohydrogen production using a hybrid artificial neural network (ANN) and response surface methodology (RSM) approach. *Environmental Progress and Sustainable Energy*, 40(1): e13485. DOI:

https://doi.org/10.1002/ep.13485

[23] Cheng, D., Ngo, H. H., Guo, W., Chang, S. W., Nguyen, D. D., Zhang, S., Deng, S., An, D. and Hoang, N. B. 2022. Impact factors and novel strategies for improving biohydrogen production in microbial electrolysis cells. *Bioresource Technology*, 346: 126588. DOI: https://doi.org/10.1016/j.biortech.2021.126588

[24] Muddasar, M., Liaquat, R., Aslam, A., Ur Rahman, M. Z., Abdullah, A., Khoja, A. H., Latif, K. and Bahadar, A. 2022. Performance efficiency comparison of microbial electrolysis cells for sustainable production of biohydrogen—A comprehensive review. *International Journal of Energy Research*, 46(5): 5625–5645. DOI: https://doi.org/10.1002/er.7606

[25] Rani, G., Banu, J. R., Kumar, G. and Yogalakshmi, K. N. 2022. Statistical optimization of operating parameters of microbial electrolysis cell treating dairy industry wastewater using quadratic model to enhance energy generation. *International Journal of Hydrogen Energy*, 47(88): 37401-37414. DOI: https://doi.org/10.1016/j.ijhydene.2022.03.120

[26] Yahya, A. M., Hussain, M. A. and Abdul Wahab, A. K. 2015. Modeling, optimization, and control of microbial electrolysis cells in a fed-batch reactor for production of renewable biohydrogen gas. *International Journal of Energy Research*, 39(4): 557–572. DOI: https://doi.org/10.1002/er.3273

[27] Dudley, H. J., Ren, Z. J. and Bortz, D. M. 2019. Competitive exclusion in a DAE model for microbial electrolysis cells. *Mathematical Biosciences and Engineering*, 17(5): 6217–6239. DOI: https://doi.org/10.48550/arXiv.1906.02086

[28] Lu, L., Vakki, W., Aguiar, J. A., Xiao, C., Hurst, K., Fairchild, M., Chen, X., Yang, F., Gu, J. and Ren, Z. J. 2019. Unbiased solar H2 production with current density up to 23 mA cm-2 by Swiss-cheese black Si coupled with wastewater bioanode. *Energy and Environmental Science*, 12(3): 1088–1099. DOI: https://doi.org/10.1039/c8ee03673j